RSC Advances

PAPER

View Article Online
View Journal | View Issue

Cite this: *RSC Adv.*, 2016, **6**, 95494

Ciprofloxacin wastewater treated by UVA photocatalysis: contribution of irradiated TiO_2 and ZnO nanoparticles on the final toxicity as assessed by *Vibrio fischeri*†

A. R. Silva,[ab] P. M. Martins,[ab] S. Teixeira,[c] S. A. C. Carabineiro,[d] K. Kuehn,[c] G. Cuniberti,[cef] M. M. Alves,[b] S. Lanceros-Mendez[agh] and L. Pereira*[b]

Photocatalysis has become an attractive process to treat wastewater since it allows a rapid and efficient degradation of micropollutants in water. A solution of ciprofloxacin (CIP) was photocatalytically treated by ultraviolet A light (UVA) and titanium dioxide (TiO_2) or zinc oxide (ZnO) nanoparticles. Toxicity of CIP and of the treated CIP solutions, as well as the toxicity of TiO_2 and ZnO irradiated nanoparticles, was evaluated towards *Vibrio fischeri*. The lowest concentration of CIP tested, 10 μg L^{-1}, leads to 50% of luminescence inhibition. Regarding irradiated nanoparticles, ZnO presented higher bacteria luminescence inhibition than TiO_2, 97 and 38%, respectively. Due to high toxicity of ZnO, it was only possible to evaluate the CIP solution treated by UVA/TiO_2. Initially, the toxicity decreased with the time of the process, but after 15 min the toxicity increased significantly (55%) and after 45 min of treatment, was 70%. High-performance liquid chromatography (HPLC) and Fourier transform infrared spectroscopy (FTIR) analysis proved that the initial decrease of toxicity was caused by CIP adsorption on catalyst surface, which latter increased due to the generation of by-products and toxicity contribution of soluble nanoparticles. Ten by-products were identified by liquid chromatography-mass spectrometry (LC-MS) and the mechanism of CIP photocatalytic degradation was proposed.

Received 29th July 2016
Accepted 26th September 2016

DOI: 10.1039/c6ra19202e

www.rsc.org/advances

1. Introduction

The use of pharmaceuticals in human and veterinary medical practices and aquaculture has led to their constant release into the environment. The persistence of such residues, namely antibiotics, in surface water is a serious concern due to their potential impact in ecosystems and public health. Even at low concentrations,[1,2] it may be a potential threat by inducing multi resistance in bacteria.[3–5] Considering that the raw sewage and wastewater effluents are a major source of micropollutants, it is important to develop effective processes to their removal during wastewater and drinking-water treatment.[6–8] CIP, in particular, is an antibiotic which tends to persist in aquatic environments.[9,10] As the elimination of CIP by conventional wastewater treatments is incomplete, additional treatments like membrane treatments[11] and advanced oxidation processes (AOPs)[12] should be performed to mitigate its undesired effects. AOPs are non-biological technologies used to remove several compounds from water and have been successfully applied to remove pharmaceuticals.[12] They are mainly based in the *in situ* production of hydroxyl radicals ($OH^{\bullet}$) with great oxidative power.[4,13,14] AOPs comprise degradation treatments such as ozonation,[9,15] photolysis,[12,16] Fenton oxidation[17] and heterogeneous photocatalysis (semiconductor photocatalysis).[12,18] Compared to other AOPs, photocatalysis is outstanding regarding the operation at ambient conditions, photochemical stability, low costs and commercially availability of catalysts.[12,17,19] Additionally, this process allows the complete mineralization of compounds.[17] The basic components for this photocatalytic process are a catalyst (typically a semiconductor), a source of photon energy (UV radiation or solar light), oxygen and water.[11,19] Several semiconductors have been studied,[17,20,21] however suspensions of TiO_2 and ZnO nanoparticles are the most commonly used in wastewater decontamination.[22,23] They are highly active,

[a]*Center/Department of Physics, University of Minho, 4710-057 Braga, Portugal*
[b]*CEB – Centre of Biological Engineering, University of Minho, 4710-057 Braga, Portugal. E-mail: lucianapereira@deb.uminho.pt*
[c]*Institute for Materials Science and Max Bergmann Center of Biomaterials, TU Dresden, 01062, Ghana*
[d]*Laboratório de Catálise e Materiais (LCM), Laboratório Associado LSRE-LCM, Faculdade de Engenharia, Universidade do Porto, 4200-465 Porto, Portugal*
[e]*Dresden Center for Computational Materials Science (DCCMS), TU Dresden, 01062 Dresden, Germany*
[f]*Center for Advancing Electronics Dresden, TU Dresden, 01062 Dresden, Germany*
[g]*BCMaterials, Parque Científico y Tecnológico de Bizkaia, 48160-Derio, Spain*
[h]*IKERBASQUE, Basque Foundation for Science, 48013 Bilbao, Spain*

† Electronic supplementary information (ESI) available. See DOI: 10.1039/c6ra19202e

chemically and thermally stable, and chemically resistant to breakdown and have strong mechanical properties.

Regarding the photocatalytic degradation of CIP, some studies using TiO_2 (ref. 5 and 24) and ZnO[25] nanoparticles under UV or solar radiation[24,26] have stated that the degradation occurs primarily at the piperazine ring originating several by-products.[9,27] With longer irradiation time, more functional groups can be removed, leading to the mineralization of the compound to innocuous carbon dioxide and water.[24,26,28] However, in spite of mineralizing a wide range of compounds, photocatalysis may not represent the optimal approach to decrease the toxicity of water contaminated with pharmaceuticals.[5,29] Toxicity assessment is a crucial step to validate degradation processes and their environmental impacts.[30] It has been shown that generated intermediates can be more toxic than their parent compounds.[31,32] Toxicity bioassays are useful tools to evaluate the toxicological potential of wastewater treated by photocatalysis. The test organisms traditionally used in bioassays, can be grouped in: algae and plants, crustaceans, fish, rotifers, annelids, molluscs and microorganisms.[33–36] *V. fischeri* has been used as sensitive biosensor with a short time of toxicity response, 15–30 min. Toxicity bioassays with these bacteria are based in the assessment of bacterial luminescence emission when exposed to toxic substances. Bioluminescence is coupled to metabolic activity. A decrease is associated with the toxicity of the tested sample, explicitly the lower light output, the higher the toxicity.[37,38]

This study is focused on the toxicity evaluation of a solution containing CIP treated by UVA/TiO_2 and UVA/ZnO. The toxicity of by-products formed during CIP photocatalytic degradation and the contribution of irradiated TiO_2 and ZnO nanoparticles on global toxicity was evaluated. To the best of our knowledge, this is the first report where the contribution of TiO_2 and ZnO nanoparticles for the global toxicity of final treated solution was assessed.

2. Experiments

2.1 Chemicals and bacteria

TiO_2 P25 (CAS 13463-67-7) was kindly provided by Evonik Industries AG; ZnO particles (CAS 1314-13-2) were obtained from Iolitec. TiO_2 P25 present nanoparticles size of 30 nm in diameter and specific surface area values, ranging between 35 to 65 $m^2\ g^{-1}$. ZnO particles size of 120 nm in diameter and specific surface area between and 4.9 to 6.8 $m^2\ mL^{-1}$.[39–41] CIP (98%) (CAS 85721-33-1) and paraformaldehyde (CAS 30525-89-4) were obtained from Sigma-Aldrich. CIP was used without further purification. A stock solution of 1 mg L^{-1} was prepared in ultra-pure water and two droplets of hydrochloric acid were added to ensure the complete solubility of CIP. Formic acid (98%) (CAS 64-18-6) was acquired from MERCK, acetonitrile (ACN, HPLC analytic grade) (CAS 75-05-8) and zinc sulfate heptahydrate ($ZnSO_4 \cdot 7H_2O$) (7446-20-0) were obtained from Panreac. 4,6-Diamidino-2-phenylindole (DAPI) (CAS 28718-90-3) was obtained from Thermo Fisher Scientific (Molecular Probes). The bioluminescent bacteria, *Vibrio fischeri* NRRL B-11177, BioFix® Lumi medium, diluent and osmotic pressure adjusting solutions were purchased from Macherey-Nagel GmbH & Co. KG (Düren, Germany).

2.2 Photocatalytic degradation of ciprofloxacin

The photoreactor set up is presented in ESI (Fig. S1, ESI†). A beaker containing 50 mL of an aqueous solution containing 300 μg L^{-1} of CIP and 1 g L^{-1} of the photocatalytic nanoparticles (TiO_2 or ZnO) was, firstly, placed in the dark for 30 minutes under magnetic stirring, in order to allow the adsorption–desorption equilibrium before starting the photocatalytic process. After that time, the beaker was placed for 45 min under UVA, intensity peak at 365 nm, previously stabilized towards an intensity value of 1.6 to 1.7 mW cm^{-2}, as measured by a luxmeter (UV34 Lux Meter-PCE). During the process, samples were withdrawn at times −30 min (before irradiation, sample t_{-30}), 0 min (sample t_0), 6 min (sample t_6), 10 min (sample t_{10}), 15 min (sample t_{15}), 30 min (sample t_{30}) and 45 min (sample t_{45}), and centrifuged during 40 min at 14 000 rpm and 21 °C, in order to remove the suspended nanoparticles.

For HPLC and LC-MS analysis, samples were filtered with a Spartan 13/0.2 RC filter pore size 0.2 μm, from Whatman TM. CIP was analyzed by HPLC, using an Ultra HPLC (Shimadzu Nexera XZ) equipped with a diode array detector (SPD-M20A), autosampler (SIL-30AC), degassing unit (DGU-20A5R), LC -30AD solvent delivery unit, and a Labsolutions software. A RP-18 endcapped Purospher Star column (250 mm × 4 mm, 5 μm particle size, from MERCK, Germany) was used. Mobile phase was composed of two solvents: 0.1% formic acid aqueous solution and ACN. Compounds were eluted at a flow rate of 0.8 mL min^{-1} and 40 °C, with an increase from 5 to 15% of ACN over 6 minutes, followed by an isocratic step during 12 minutes, then from 15% to 40% of ACN during 12 minutes, condition maintained for 10 minutes. A calibration curve at increasing CIP concentrations (0 and 300 μg L^{-1}) was made. The calibration curves presented linearity in the range evaluated with correlation coefficients, R^2, higher than 0.990. The estimated detection limit of the equipment was 19.33 μg L^{-1}.

FTIR of the dried TiO_2 nanoparticles, withdrawn during the photocatalytic process at t_0, t_{15} and t_{45}, were performed in an ALPHA FTIR spectrometer (Bruker) over a range of 650–4000 cm^{-1}, using 64 scans with a resolution of 4 cm^{-1}. The spectra were obtained with Bomem softwareGRAMS/LT (v 7.0) – (Thermo Galactic).

2.3 Identification of the by-products of ciprofloxacin photocatalysis

The by-products generated during CIP photocatalytic degradation were identified by LC-MS. Samples were separated on an HPLC Accela system (Thermo Fischer Scientific, Bremen, Germany) using a Kinetex XB-C18 column (Phenomenex. 1.7 μm particle size and dimensions 2.1 mm ID × 100 mm). Gradient elution was applied using 10 mM ammonium acetate adjusted to pH 2.5 with formic acid as solvent A, and methanol with 0.1% formic acid (v/v) as solvent B. The mobile phase composition (A : B, v/v) was 80 : 20 at 0 min, 50 : 50 at 10 min, 10 : 90 at 13 min, which was kept unchanged until 14 minutes of elution and

then, 0 : 100 at 14 : 50 until 16 min, followed by column re-equilibration at condition 80 : 20 from 17 to 20 min. Sample trays were kept at 4 °C and the flow rate was of 150 μL min^{-1}. The MS analysis were done on an LTQ Orbitrap™ XL hybrid mass spectrometer (Thermo Fischer Scientific, Bremen, Germany) controlled by LTQ Tune Plus 2.5.5 and Xcalibur 2.1.0. The capillary voltage of the electrospray ionization source (ESI) was set to 3.5 kV. The capillary temperature was 300 °C. The sheath gas and auxiliary gas flow rate were at 40 and 10 (arbitrary unit as provided by the software settings). The capillary voltage was 26 V and the tube lens voltage 80 V. MS data handling software (Xcalibur QualBrowser software, Thermo Fischer Scientific, Bremen, Germany) was used to search for predicted metabolites by their mass-to-charge (*m*/*z*) value. The *m*/*z* ratios were obtained in positive mode and all peaks were checked for *m*/*z* values.

2.4 *Vibrio fischeri* characterization

V. fischeri morphology was assessed by epifluorescence microscopy using a bacteria concentration of 10^8 cells per mL to facilitate their observation. Furthermore, in order to estimate the bacteria average size and distribution, they were fixed, dehydrated and stained. For this purpose, 1 mL of bacteria culture was centrifuged at 10 000 rpm, during 5 min at room temperature, 500 μL of supernatant were removed and the bacteria pellet was re-suspended. Next, 500 μL of 4% (w/v) paraformaldehyde was added and kept for 60 minutes at room temperature to fix the cells. For bacteria dehydration, samples were centrifuged again at 10 000 rpm, during 5 min, at room temperature and 500 μL of 50% (v/v) ethanol was added for 30 min before staining. With respect to staining, the alcoholic bacteria suspension was centrifuged at 10 000 rpm for 5 min at room temperature. The bacteria pellet was placed on the microscope slide, stained with DAPI and kept in the dark for 10 min. Microscopic analysis were performed in an epifluorescence microscope (Olympus BX51) coupled with a DP72 digital camera and equipped with a filter set (DAPI-365-370/421). The statistical analysis was performed with a total number of 70 cells.

For the emission spectrum, *V. fischeri* was placed in a microplate reader Biotek® Cytation3 in spectrum mode, using a Gen5 Data Analysis software integrated with a BioTek imaging and detection system using the Olympus Cellsense software.

2.5 Toxicity assays

Toxicity analysis were performed with a bioassay using *V. fischeri*, according to the standard ISO 11348-3, "water quality – determination of the inhibitory effect of water samples on the light emission of *V. fischeri* (luminescent bacteria test)",[42] using the method freeze-dried bacteria. The bacteria concentration used in the tests was 1.5×10^6 cells per mL instead of the concentration proposed in the ISO 11348-3 (1.5×10^6 cells per mL). This change was based in the study of luminescence intensity with increasing cells concentration (Fig. S2, ESI†). $ZnSO_4 \cdot 7H_2O$ was used as a positive control as described in ISO 11348-3.

The luminescence assays were carried out in a microplate reader Biotek® Cytation3, using a 96 well optical Btm Plt polymer base Blk plate, from Nalge Nunc™ International. Samples were prepared in eppendorfs of 1 mL according to the ISO 11348-3, but a volume of 200 μL was transferred for the microplates for reading. The intensity of luminescence was read at different contact times (Ct) between the bacteria and the samples to be evaluated: 0 min (Ct_0), 15 min (Ct_{15}) and 30 min (Ct_{30}). Samples evaluated include the solutions of CIP after UVA/TiO_2 treatment at increasing degradation times (t_0 to t_{45}); TiO_2 and ZnO irradiated nanoparticles at increasing irradiation times (t_0 to t_{90}) and solutions of increasing concentrations of CIP (10 to 1000 μg L^{-1}). The Ct_0 corresponds to the luminescence intensity measured immediately after the contact between the bacteria's suspension and the samples. The toxicity evaluation of the samples is based on the luminescence inhibition (INH%) caused by the presence of potentially toxic samples to the bacteria (eqn (1)).[43,44]

$$\mathrm{INH\%} = 100 - \left(\frac{\mathrm{IT_T}}{\mathrm{KF} \times \mathrm{IT_0}}\right) \times 100, \text{ with } \mathrm{KF} = \frac{\mathrm{IC_T}}{\mathrm{IC_0}} \quad (1)$$

where KF is the correction factor and characterizes the natural loss of luminescence of the control; IC_0 is the initial luminescence intensity of the control sample; IT_0, the luminescence intensity of the tested sample, immediately before the addition of the tested sample at the time 0; IC_T is the luminescence intensity of the control after the contact time and IT_T is the luminescence intensity of the sample after the contact time.

For the evaluation of the toxicity exerted by the nanoparticles, a solution containing 1 g L^{-1} of nanoparticles was prepared in ultra-pure water at a final volume of 50 mL. The solution was placed under UVA radiation (365 nm) for increasing irradiation times (0–45 min). Samples were centrifuged before analysis to remove nanoparticles. All the assays were performed in triplicate.

3. Results and discussion

3.1 Photocatalytic degradation of ciprofloxacin

Photocatalytic degradation of CIP was evaluated by HPLC at degradation times −30, 0, 6, 15, 30 and 45 min. CIP was detected at 275 nm with a retention time (Rt) of 13.2 min (Fig. 1). HPLC results indicate the presence of CIP in the sample t_{-30}, for both catalysts, with an estimated concentration of 266.12 for ZnO and 285.68 μg L^{-1} for TiO_2 (Table S1, ESI†). At the degradation time t_0, CIP concentration in solution treated by ZnO nanoparticles was 97.59 μg L^{-1} and by TiO_2 nanoparticles was 42.36 μg L^{-1}, representing a decrease of CIP in solution of ~63% and ~85% for ZnO and TiO_2 nanoparticles, respectively. In sample t_6, CIP was no longer detected in the treated solution. The abrupt decrease in CIP concentration in the first 30 minutes of the process without UVA, is addressed to the adsorption of CIP onto the nanocatalyst surface.[45] The higher adsorption exhibited by TiO_2 nanoparticles regarding ZnO nanoparticles is consistent with their specific surface area values, ranging between 35 to 65 m^2 g^{-1} for TiO_2 (ref. 41) and 4.9 to 6.8 m^2 g^{-1} for ZnO.[39] On the other hand, the decrease of CIP

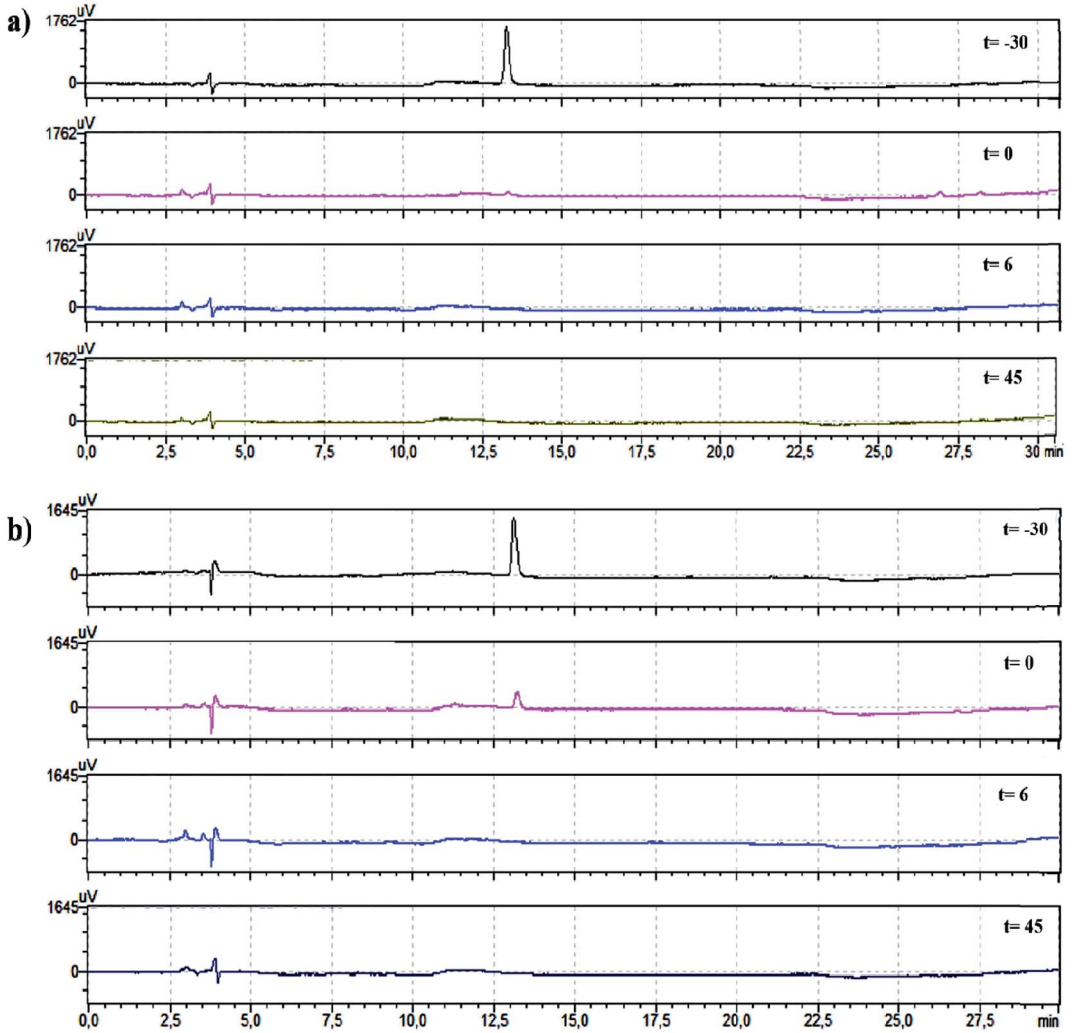

Fig. 1 HPLC analysis of CIP degraded samples with ZnO nanoparticles (a) and TiO_2 nanoparticles (b) at degradation times −30, 0, 6 and 45 min.

from t_0 to t_6 occurs due to the photocatalytic activity by UVA. Other authors have reported about the efficiency of both catalysts in the degradation of micropollutants, which is highly dependent on compound and catalyst characteristics. For instance, Evgenidou *et al.* (2005) studying the degradation of dichlorvos, have obtained higher efficiency with TiO_2 than with ZnO.[46] In contrast, for example, photocatalytic degradation of an azo dye was more efficient with ZnO than with TiO_2.[47]

In order to evaluate the adsorption of CIP on TiO_2 nanoparticles surface, the recovered nanoparticles at degradation times t_0, t_{15} and t_{45} were analyzed by FTIR (Fig. 2). The FTIR spectrum of TiO_2 nanoparticles shows an absorbance broad band at 3750–3000 cm^{-1} related with the stretching hydroxyl (O–H), which represents the water as moisture. Also, the characteristic band of TiO_2 was found at 1635 cm^{-1}, indicating the stretching of titanium carboxylate which is in accordance with the literature.[48,49] Additionally, the CIP characteristic absorption band at 2950.5 cm^{-1} is displayed. This is in agreement with other works that report a band at 3000–2950 cm^{-1}, representing the alkene and aromatic C–H stretching. The C–H stretching vibration of the cyclopropyl group is also responsible for this band.[50] FTIR analyses were not performed with ZnO nanoparticles as the high solubility of these nanoparticles did not allow recovering the required amount for analysis.

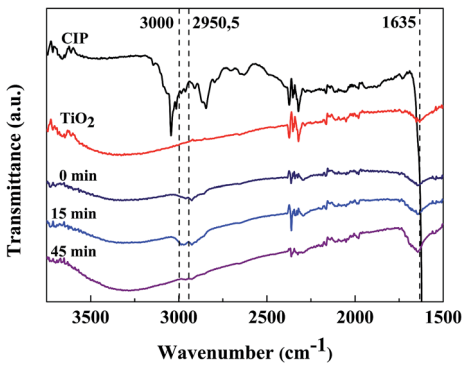

Fig. 2 FTIR analysis of CIP, TiO_2 nanoparticles and recovered TiO_2 nanoparticles after CIP photocatalytic degradation times 0, 15 and 30 minutes.

The CIP characteristic band at 2950.5 cm^{-1} shows an increasing intensity of the nanoparticles recovered from treated samples from t_0 to t_{15}, indicating that the amount of CIP adsorbed onto nanoparticles surface increased. At the degradation time of t_{45}, this band disappeared, signifying that there was no more antibiotic adsorbed on the catalysts' surface. Therefore, the results from FTIR analysis are consistent with those obtained by HPLC. It is possible to establish an inverse relation between the decrease of CIP in solution, assessed by HPLC, and an increase of the amount of CIP on the catalysts' surface, by FTIR. At t_0, HPLC analysis indicated a decrease of CIP in solution and FTIR analysis of the recovered nanoparticles at that time, showed the presence of CIP on its surface, pointing out that the decrease of CIP in solution was caused by adsorption onto the particles surface. In samples t_6, t_{15}, t_{30} and t_{45} CIP was not detected in the solution, as monitored by HPLC. However, FTIR results of the nanoparticles recovered at irradiation times (0, 6, 15, 30 and 45 min) showed an increase in the intensity of the characteristic band of CIP at irradiation times from 0 to 15 min, revealing increasing adsorption of the antibiotic at those times. This explains the non-detection of CIP in the solution at t_6 by HPLC. Probably, during this 15 min of reaction two processes are occurring at the same time: adsorption onto nanoparticles and photocatalytic degradation. At t_{45}, CIP was not detected in solution, by HPLC, nor on the nanoparticles surface, by FTIR, showing a complete photocatalytic degradation of the antibiotic and proving that UVA/TiO_2 photocatalysis is an efficient approach to remove CIP from contaminated water.

3.2 Identification of by-products of CIP photocatalytic degradation

LC-MS analyses were performed in order to identify CIP photocatalytic degradation products. These by-products may result from the reaction at specific sites of CIP, such as the piperazine ring and the quinolone moieties by hydroxyl radicals.[26] Regarding the *m*/*z* ratios obtained in positive mode, 7 structures were identified for samples degraded in the presence of TiO_2 and 9 with ZnO (Tables S2 and S3, ESI†). Therefore, a mechanism of CIP photocatalytic degradation is proposed (Fig. 3a and b). The mechanism of CIP degradation was similar for both catalysts and followed two routes. One starts with the loss of a fluorine ion, yielding the molecular ion *m*/*z* 313 corresponding to product 1 (P1), followed by the loss of the piperazine ring (P2, *m*/*z* 244). The molecular ion at *m*/*z* 330 was also found, and may result from the insertion of an OH group, which can also lead to the compound P2, by losing the piperazine ring and the OH. Compound P2 is further degraded, losing CO or C_3H_4, originating the molecular ions *m*/*z* 217 (P3) and *m*/*z* 205 (P4), respectively. Additionally, the molecular ion *m*/*z* 186 (P5) was identified in samples degraded by TiO_2, which results from the loss of NH and COO by P2 and the molecular ion 231 (P5′) in samples degraded by ZnO, due to the loss of NH by P2. In the other route, CIP receives an H_2O molecule and loses the piperazine ring originating the molecular ion *m*/*z* 279 (P6) which is further degraded losing the C_3H_4 (compound P7, *m*/*z* 239) or the fluorine and an OH group (compound P2, *m*/*z* 244). In samples degraded by ZnO, two other compounds (*m*/*z* 223, P8 and *m*/*z* 288, P9) were also identified. P9 results from the loss of an OH by P7 and P9 results from the loss of a COO group by CIP. The molecular structures of the identified compounds were assigned to $C_{17}H_{19}N_3O_3$ (P1), $C_{13}H_{12}N_2O_3$ (P2), $C_{12}H_{12}N_2O_2$ (P3), $C_{10}H_8N_2O_3$ (P4), $C_{12}H_{11}NO$ (P5), $C_{13}H_{12}NO_3$ (P5′), $C_{13}H_{11}N_2O_4F$ (P6), $C_{10}H_7N_2O_4F$ (P7), $C_{10}H_7N_2O_3F$ (P8) and $C_{16}H_{18}N_3OF$ (P9). Results are in accordance with previous reports stating that CIP photocatalytic degradation occurs primarily at the piperazine ring.[9,27,28]

3.3 Bacteria characterization

The results of the bacteria stained with DAPI (Fig. 4a and b) showed that it present a significant size variation ranging from 1.5 to 4.5 μm (Fig. 4c), which is in good agreement with the work developed by Ruby *et al.* (1993).[51]

Fig. S2 (ESI†), shows that light emission of bacteria depends on factors, such as cell concentration and nutrients availability in solution, which is in good agreement with the work of S. Scheerer *et al.*[37]

The bacteria emission spectrum was obtained approximately 2 h after activation in culture medium. Fig. 4d represents the emission spectrum of *V. fischeri*. The luminescence emission is a broad peak ranging between 425 to ~600 nm and the maximum luminescence was observed approximately at 490 nm, which is in accordance with literature.[52,53]

3.4 Toxicity assays

3.4.1 Toxicity of UVA irradiated nanoparticles. The toxicity caused only by TiO_2 and ZnO nanoparticles that remains in aqueous solution after the UVA photocatalytic treatment was assessed at different irradiated times. The assays were performed with the irradiated samples at different Ct with the bacteria, Ct_0, Ct_{15} and Ct_{30}, and the results are presented in Fig. 5a and b. At Ct_0, the luminescence inhibition caused for the different times of irradiation, over 45 min, has ranged between 16 and 39% and 18 to 54%, for ZnO and TiO_2 nanoparticles, respectively. After 15 minutes of Ct, the toxicity of the ZnO samples increased and ranged from 83 to 95% of inhibition. At Ct_{30}, the ZnO toxicity continued to increase until no luminescence was detected. Instead, TiO_2 nanoparticles displayed a lower luminescence inhibition, varying between 30 to 48%. According to these results, the solution obtained by ZnO/UVA is considered "very toxic". TiO_2 did not show a significant toxicity increase for all the tested samples, being "slightly toxic".[33,54,55] Further, for TiO_2 samples with reduced irradiation time, until 20 min, there is no significant variation on luminescence inhibition between the different Ct. However, with increasing irradiation time, above 40 min, the luminescence inhibition differences increases between different Ct. During the photocatalytic process, nanoparticles are exposed to UVA and this irradiation may interfere with the nanoparticles surface properties and influence the toxicity. Therefore, for water treatment by photocatalysis the study of the toxicity caused by irradiated nanoparticles has particular relevance. Previous studies were devoted

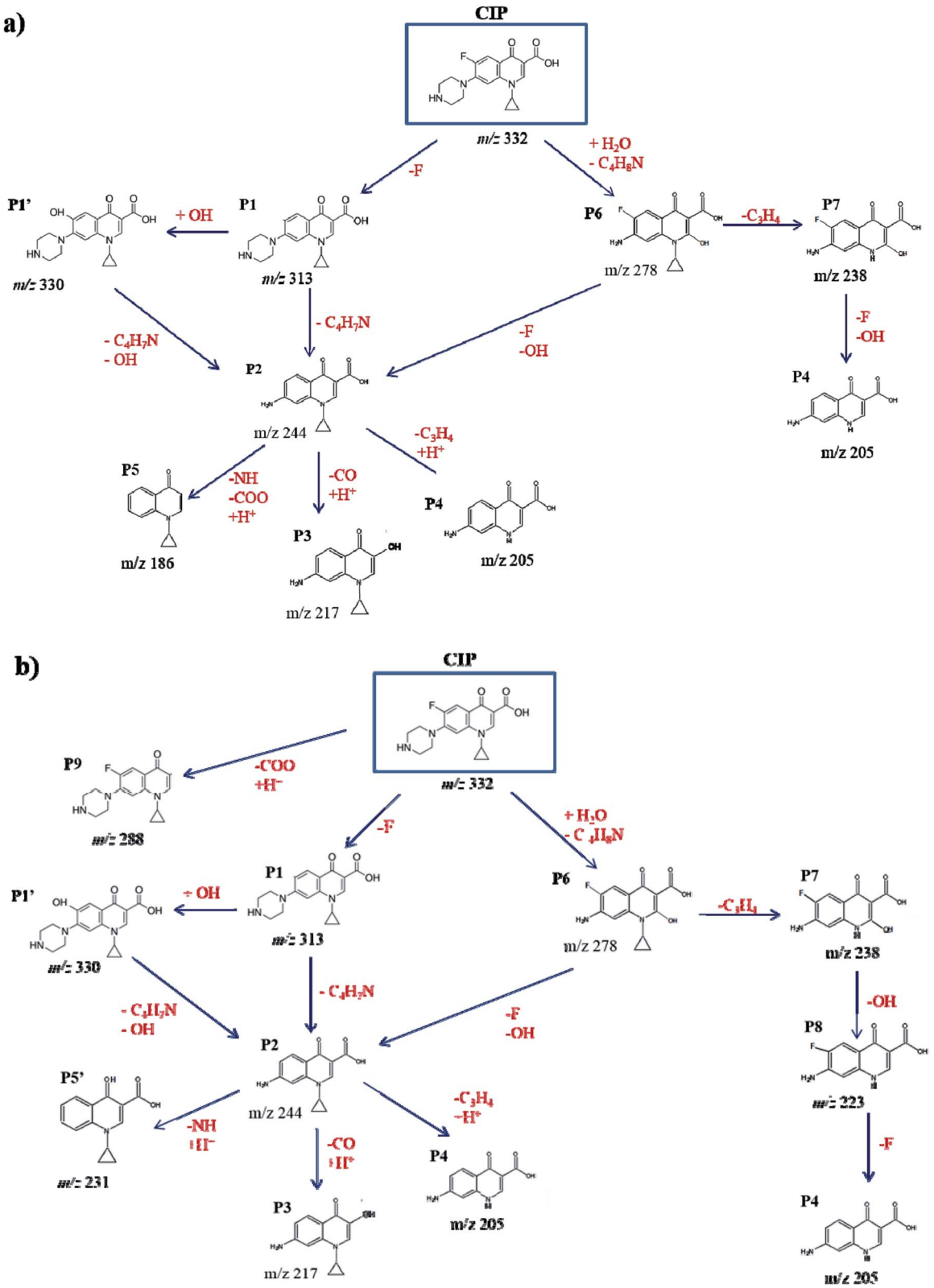

Fig. 3 Degradation mechanism of CIP photocatalytic degradation after 45 minutes of process with: (a) TiO_2 and (b) ZnO nanoparticles. P1–P9 match the products assigned to the corresponding molecular ions.

to ZnO and TiO_2 toxicity assessment in direct contact with the bacteria. The results showed that these nanoparticles promote cytotoxicity in *V. fischeri* and other organisms, such as *T. platyurus* and *Daphnia magna*.[44] The photo-induced reactive oxygen species (ROS) produced have the ability to oxidize organic contaminants and cause fatal damages in microorganisms.[20,56]

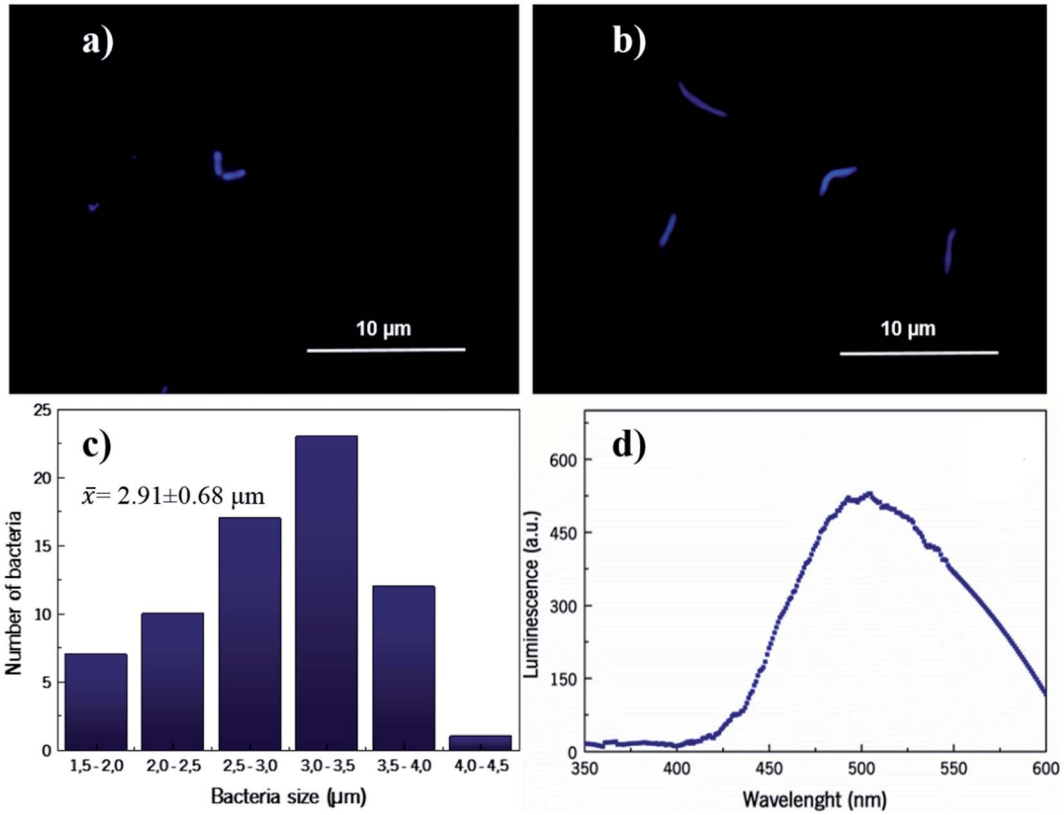

Fig. 4 (a and b) Fluorescence microscopy images of *Vibrio fischeri* cells labeled with DAPI; (c) bacterium size distribution histogram ($n = 70$) and (d) *Vibrio fischeri* emission spectrum.

Additionally, studies with crustaceans and fungi, showed that ZnO has a higher toxic effect than TiO_2.[44,57] The high toxicity of ZnO is probably related to dissolution of ZnO nanoparticles into ionic species (Zn^{2+}), which together with the ROS species produced on the nanoparticles surface, under UVA irradiation, will play a synergetic role in the enhanced toxicity towards TiO_2 nanoparticles.[44,46] The ionic species yielded by ZnO easily destabilize bacteria membrane and homeostasis. With respect to TiO_2 nanoparticles, published works revealed good stability during the irradiation time.[17]

The concentration of nanoparticles used in this study was 1.0 g L^{-1} for both catalysts, the same as used in the photocatalytic degradation of CIP. However, other studies, reported EC_{50} values of 1.9 mg L^{-1} for ZnO and 20 g L^{-1} for TiO_2, after 30 min of bacteria contact, but all those studies concern non-irradiated nanoparticles.[35,44,46] Therefore, our findings draw attention to the effect of irradiated catalysts that remain in the treated wastewaters by UVA photocatalytic processes on the final toxicity, which must be taken into account when using non immobilized catalysts.

3.4.2 Toxicity of CIP. To evaluate the effect of CIP, toxicity of solutions with increasing concentrations between 10 and 1000 μg L^{-1}, were tested. Fig. 6 a shows the luminescence inhibition caused in *V. fischeri* at Ct_0 and Ct_{30}. As can be seen, the profile and extent of luminescence inhibition at Ct_0 and Ct_{30} is similar. The results show that CIP presents high toxicity

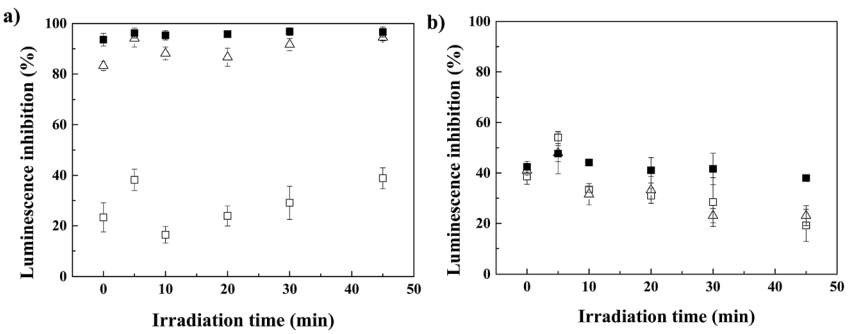

Fig. 5 Luminescence inhibition of *Vibrio fischeri* caused by irradiated ZnO (a) and TiO_2 (b) nanoparticles. (□), Ct_0; (△), Ct_{15} and (■), Ct_{30}.

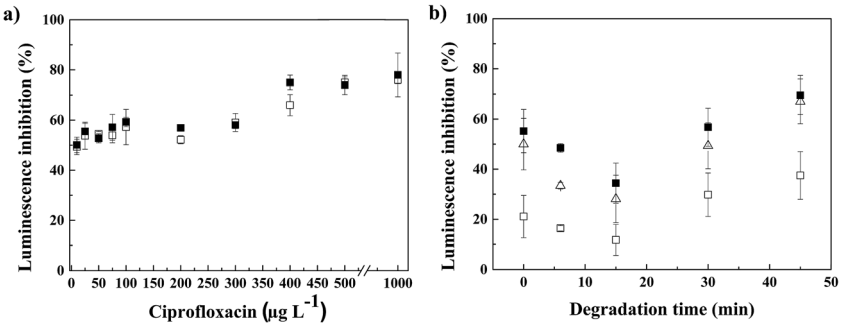

Fig. 6 Luminescence inhibition of *Vibrio fischeri* caused by increasing CIP concentrations (a) and treated CIP solution by UVA/TiO_2 (b), at different contact times. (□), Ct_0; (△), Ct_{15} and (■), Ct_{30}.

towards *V. fischeri* with all the concentrations tested. At the lowest concentration, 10 μg L^{-1}, *V. fischeri* luminescence inhibition was ~50%. Inhibition increased to 60% with the increase of CIP concentration until 100 μg L^{-1}, which was maintained for concentrations until 300 μg L^{-1}, but for higher amounts (400 to 1000 μg L^{-1}) the inhibition increases up to ~80%. Relatively to other studies, the concentration that caused 50% of luminescence inhibition found in this work is considerably lower. For instance, Hernando *et al.* (2007) found an EC_{50} value for CIP of 5.9 mg L^{-1} during an exposure to *V. fischeri* of 30 minutes.[58] Nevertheless, as mentioned before, the bacteria response depends on other variables, such as cells concentration and medium nutrients. In this study, a higher concentration of bacteria (1.5×10^6 cell per mL) was used to obtain better luminescent signal. With high bacteria concentration there is greater competition for nutrients in the medium. This competition together with the antibiotic toxicity may explain the lower EC_{50} value. Indeed, to evaluate the bacteria behavior when exposed to a toxic reference substance ($ZnSO_4 \cdot 7H_2O$), different concentrations of *V. fischeri* were tested. Results have shown that for cell concentrations between 1.0×10^6 to 2.5×10^6 cell per mL the luminescence decay rate increased from 0.081 ± 0.003 to 0.159 ± 0.014 min^{-1}, respectively (Fig. S3, ESI†). This indicates that increasing bacteria concentration increases the decay rate in the luminescence signal.

3.4.3 Toxicity of CIP solution treated by UVA/TiO_2 photocatalysis. Due to the high solubility and high toxicity caused by irradiated ZnO nanoparticles, luminescence inhibition assays could only be performed for CIP samples degraded with TiO_2 nanoparticles. Results are presented in Fig. 6b.

A decrease of luminescence inhibition of the treated CIP samples (initial concentration 300 μg L^{-1}) was observed from degradation t_0 to t_{15}. However, for higher degradation times, the toxicity increased reaching the maximum of luminescence inhibition at t_{45}. Additionally, the luminescence inhibition increased with the increase of Ct, reaching the maximum values at Ct_{30}. Based on the obtained results, after 15 min of photocatalytic degradation, the sample can be considered "*slightly toxic*" and the samples corresponding to degradation times of 30 and 45 minutes considered "*very toxic*".[33,54] Toxicity results are consistent with HPLC and FTIR analysis. From the degradation t_0 to t_{15}, toxicity decreased as the antibiotic was adsorbed on nanoparticles and, consequently, degraded. Additionally, LC-MS analysis have shown that most of the products were already present in the first 15 min of reaction, proving that adsorbed CIP was simultaneously degraded (Fig. S4, ESI†). However, at those treatment times, the concentration of by-products may be too low to affect the bacteria. As the photocatalysis proceeded, increasing concentration of formed by-products lead to the abrupt increase of toxicity, which was higher at t_{45} of treatment. The results have shown that the CIP solutions after UVA/TiO_2 degradation are more toxic than the original compound. Some studies concerning electrochemical degradation support the herein obtained results, reporting a drastic increase of toxicity after 20 minutes of treatment, which is probably caused by the formation of highly toxic by-products.[59,60] However, the toxicity of the treated solution comprises not only the by-products but also the contribution of irradiated TiO_2 nanoparticles, as stated before. Indeed, considering the 38% obtained merely with TiO_2, the by-products exerted only 32% of inhibition which is low than the initial 55% caused by 300 μg L^{-1}.

4. Conclusions

This work demonstrates that photocatalysis, using UVA and TiO_2 and ZnO nanocatalysts, is an efficient process to remove 300 μg L^{-1} of CIP from water in less than 6 minutes. Additionally, the toxicity of the catalytic nanoparticles and the potential toxicity of CIP by-products, towards *Vibrio fischeri*, was also addressed. With respect to nanoparticles toxicity, the results showed that ZnO nanoparticles irradiated with UVA are "*highly toxic*", causing 97% of bacteria luminescence inhibition. TiO_2 nanoparticles are considered "*slightly toxic*", displaying 49% of luminescence inhibition. Testing increasing CIP concentrations, it was found that 10 μg L^{-1} caused 50% of bacteria luminescence inhibition, after 30 minutes of contact. Considering the photocatalytic treatment of CIP model wastewater, combining UVA and TiO_2 nanoparticles, HPLC and FTIR analysis confirm that the initial decrease of toxicity was caused by CIP adsorption on catalyst surface and the toxicity increases as increasing the degradation time, due to by-products formation. Moreover, samples treated during 45 min presented superior luminescence inhibition (70%) than in the begging of

the process (55%), indicating that instead of detoxification, photocatalytic process increased the toxicity of the solution, due to the contribution of by-products and soluble irradiated catalysts. Finally, with respect to identification of CIP by-products during 45 min of treatment, ten compounds were identified and the mechanism of CIP photocatalytic degradation was proposed.

This work indicates that through the photocatalytic process using TiO_2 or ZnO nanoparticles is effective to degrade CIP, the toxicity introduced by by-products and, especially, by the irradiated nanoparticles, may be a limitation. Increasing degradation time will provide further insights about by-products fate and their toxicity.

Acknowledgements

This study was supported by the Portuguese Foundation for Science and Technology (FCT) under the scope of the strategic funding of UID/BIO/04469/2013 and UID/FIS/04650/2013 and COMPETE 2020 (POCI-01-0145-FEDER-006684) and BioTecNorte operation (NORTE-01-0145-FEDER-000004) funded by European Regional Development Fund under the scope of Norte2020 – Programa Operacional Regional do Norte. P. M. Martins holds an FCT grant SFRH/BD/98616/2013 and Luciana Pereira a post-doc fellowship (SFRH/BPD/110235/2015). SACC thanks FCT for investigator FCT program (IF/01381/2013/CP1160/CT0007), with financing from the European Social Fund and the Human Potential Operational Program. The authors thank financial support from the Basque Government Industry Department under the ELKARTEK Program. A. R. Silva thanks to Diana Vilas Boas, for the support in microscopy techniques. Authors are thankful to Dr Carlos Sá (CEMUP) for assistance with LC-MS analyses and to Dr Ana Rita Lado Ribeiro (LCM) for the help given through information sharing and discussions. S. Teixeira thanks the ESF for funding the project 'InnoMedTec' and the 'Alfred Kaercher Foerderstiftung'for financial support. K. Kuehn thanks BMBF funding NaViTex under the CLIENT program (02WCL1264A).

References

1 OECD, *Health at a Glance 2013: OECD Indicators*, OECD Publishing, 2013.
2 K. Kümmerer, in *Pharmaceuticals in the Environment: Sources, Fate, Effects and Risks*, Springer Science & Business Media, second, 2013, p. 527.
3 M. Sui, S. Xing, L. Sheng, S. Huang and H. Guo, *J. Hazard. Mater.*, 2012, **227–228**, 227–236.
4 G. Lofrano, M. Carotenuto, C. S. Uyguner-Demirel, A. Vitagliano, A. Siciliano and M. Guida, *Environ. Technol.*, 2013, **35**, 1234–1242.
5 T. Paul, M. C. Dodd and T. J. Strathmann, *Water Res.*, 2010, **44**, 3121–3132.
6 C. Pablos, J. Marugán, R. Van Grieken and E. Serrano, *Water Res.*, 2013, **47**, 1237–1245.
7 S. Teixeira, R. Gurke, H. Eckert, K. Kühn, J. Fauler and G. Cuniberti, *J. Environ. Chem. Eng.*, 2015, 12.
8 P. M. Martins, R. Miranda, J. Marques, C. J. Tavares, G. Botelho and S. Lanceros-Mendez, *RSC Adv.*, 2016, **6**, 12708–12716.
9 C. Liu, V. Nanaboina, G. V Korshin and W. Jiang, *Water Res.*, 2012, **46**, 5235–5246.
10 C. Fogarty, *Photocatalytic Oxidation of Ciprofloxacin Under UV-LED Light*, PhD thesis, Worcester Polytechnic Institute, 2013, p. 40.
11 V. Homem and L. Santos, *J. Environ. Manage.*, 2011, **92**, 2304–2347.
12 M. Klavarioti, D. Mantzavinos and D. Kassinos, *Environ. Int.*, 2009, **35**, 402–417.
13 T. An, H. Yang, G. Li, W. Song, W. J. Cooper and X. Nie, *Appl. Catal., B*, 2010, **94**, 288–294.
14 H. Yang, T. An, G. Li, W. Song, W. J. Cooper, H. Luo and X. Guo, *J. Hazard. Mater.*, 2010, **179**, 834–839.
15 M. Mehrjouei, S. Müller and D. Möller, *Chem. Eng. J.*, 2014, **263**, 209–219.
16 I. Michael, L. Rizzo, C. S. McArdell, C. M. Manaia, C. Merlin, T. Schwartz, C. Dagot and D. Fatta-Kassinos, *Water Res.*, 2013, **47**, 957–995.
17 R. V. Prihod and N. M. Soboleva, *J. Chem.*, 2013, **2013**, 8.
18 C. Wang, H. Liu and Y. Qu, *J. Nanomater.*, 2013, **2013**, 14.
19 C. J. Philippopoulos and M. D. Nikolaki, in *New Trends in Technologies*, ed. B. Ramov, INTECH, 2010, p. 242.
20 M. N. Chong, B. Jin, C. W. K. Chow and C. Saint, *Water Res.*, 2010, **44**, 2997–3027.
21 L. Pereira, R. Pereira, C. S. Oliveira, L. Apostol, M. Gavrilescu, M.-N. Pons, O. Zahraa and M. M. Alves, *Photochem. Photobiol.*, 2013, **89**, 33–39.
22 M. R. Hoffmann, S. T. Martin, W. Choi and D. W. Bahnemannt, *Chem. Rev.*, 1995, **95**, 69–96.
23 M. da Motta, R. Pereira, M. Madalena Alves and L. Pereira, *Water Sci. Technol.*, 2014, **70**, 1670–1676.
24 M. Sturini, A. Speltini, F. Maraschi, A. Profumo, L. Pretali, E. A. Irastorza, E. Fasani and A. Albini, *Appl. Catal., B*, 2012, **119–120**, 32–39.
25 M. El-Kemary, H. El-Shamy and I. El-Mehasseb, *J. Lumin.*, 2010, **130**, 2327–2331.
26 J. C. Durán-Álvarez, E. Avella, R. M. Ramírez-Zamora and R. Zanella, *Catal. Today*, 2016, 266, 175–187.
27 A. S. Maia, A. R. Ribeiro, C. L. Amorim, J. C. Barreiro, Q. B. Cass, P. M. L. Castro and M. E. Tiritan, *J. Chromatogr. A*, 2014, **1333**, 87–98.
28 H.-G. Guo, N.-Y. Gao, W.-H. Chu, L. Li, Y.-J. Zhang, J.-S. Gu and Y.-L. Gu, *Environ. Sci. Pollut. Res. Int.*, 2013, **20**, 3202–3213.
29 *Pharmaceuticals in drinking-water*, World Health Organization, France, 2012.
30 L. Duester, M. Burkhardt, A. C. Gutleb, R. Kaegi, A. Macken, B. Meermann and F. von der Kammer, *Front. Chem.*, 2014, **2**, 39.
31 A. L. Giraldo, G. a. Peñuela, R. a. Torres-Palma, N. J. Pino, R. a. Palominos and H. D. Mansilla, *Water Res.*, 2010, **44**, 5158–5167.
32 L. Rizzo, S. Meric, D. Kassinos, M. Guida, F. Russo and V. Belgiorno, *Water Res.*, 2009, **43**, 979–988.

33 E. Mendonça, A. Picado, S. M. Paixão, L. Silva, M. A. Cunha, S. Leitão, I. Moura, C. Cortez and F. Brito, *J. Hazard. Mater.*, 2009, **163**, 665–670.
34 L. Rizzo, *Water Res.*, 2011, **45**, 4311–4340.
35 D. Minetto, G. Libralato and A. Volpi Ghirardini, *Environ. Int.*, 2014, **66**, 18–27.
36 J. Marugán, D. Bru, C. Pablos and M. Catalá, *J. Hazard. Mater.*, 2012, **213–214**, 117–122.
37 S. Scheerer, F. Gomez and D. Lloyd, *J. Microbiol. Methods*, 2006, **67**, 321–329.
38 T. Backhaus and L. H. Grimme, *Chemosphere*, 1999, **38**, 3291–3301.
39 *Zinc Oxide Technical Data Sheet*, Iolitec nanomaretials, 2009, p. 5.
40 *AEROXIDE®, AERODISP® and AEROPERL® Titanium Dioxide as Photocatalyst*, Evonik industries, 2015, pp. 4–11.
41 X.-T. Zhou, H.-B. Ji and X.-J. Huang, *Molecules*, 2012, **17**, 1149–1158.
42 ISO 11448-3, 2007.
43 S. Parvez, C. Venkataraman and S. Mukherji, *Environ. Int.*, 2006, **32**, 265–268.
44 M. Heinlaan, A. Ivask, I. Blinova, H.-C. Dubourguier and A. Kahru, *Chemosphere*, 2008, **71**, 1308–1316.
45 X. Van Doorslaer, K. Demeestere, P. M. Heynderickx, H. Van Langenhove and J. Dewulf, *Appl. Catal., B*, 2011, **101**, 540–547.
46 E. Evgenidou, K. Fytianos and I. Poulios, *Appl. Catal., B*, 2005, **59**, 81–89.
47 S. Sakthivel, B. Neppolian, M. V Shankar, B. Arabindoo, M. Palanichamy and V. Murugesan, *Sol. Energy Mater. Sol. Cells*, 2003, **77**, 65–82.
48 M. M. Ba-abbad, A. A. H. Kadhum, A. B. Mohamad, M. S. Takriff and K. Sopian, *Int. J. Electrochem. Sci.*, 2012, **7**, 4871–4888.
49 H. Guo, K. Lin, Z. Zheng, F. Xiao and S. Li, *Dyes Pigm.*, 2012, **92**, 1278–1284.
50 S. Sahoo, C. K. Chakraborti, S. C. Mishra, U. Nath and S. Naik, *Int. J. Pharm. Sci.*, 2011, **3**, 0975–1491.
51 E. G. Ruby and L. M. Asato, *Microbiology*, 1993, **159**, 160–167.
52 J. Engebrecht, K. Nealson and M. Silverman, *Cell*, 1983, **32**, 773–781.
53 E. A. Meighen, *Luminescence*, 1999, **14**, 3–9.
54 A. R. Fernández-alba, M. D. Hernando, L. Piedra and Y. Chisti, *Anal. Chim. Acta*, 2002, **456**, 303–312.
55 K. Hund-Rinke and M. Simon, *Environ. Sci. Pollut. Res. Int.*, 2006, **13**, 225–232.
56 Y.-N. Chang, M. Zhang, L. Xia, J. Zhang and G. Xing, *Materials*, 2012, **5**, 2850–2871.
57 K. Kasemets, A. Ivask, H.-C. Dubourguier and A. Kahru, *Toxicol. In Vitro*, 2009, **23**, 1116–1122.
58 M. D. Hernando, S. De Vettori, M. J. Martínez Bueno and a. R. Fernández-Alba, *Chemosphere*, 2007, **68**, 724–730.
59 E. De Bel, J. Dewulf, B. De Witte, H. Van Langenhove and C. Janssen, *Chemosphere*, 2009, **77**, 291–295.
60 M. Diagne, N. Oturan and M. a. Oturan, *Chemosphere*, 2007, **66**, 841–848.